Microchimica Acta (2018) 185: 260
https://doi.org/10.1007/s00604-018-2798-2

ORIGINAL PAPER

A signal-on ratiometric fluorometric heparin assay based on the direct interaction between amino-modified carbon dots and DNA

Jianyong Huang[1] · Fenglan Li[2] · Rubin Guo[2] · Yuyuan Chen[2] · Zhenzhen Wang[2] · Chengfei Zhao[2] · Yanjie Zheng[2] · Shaohuang Weng[2] · Xinhua Lin[2]

Received: 20 December 2017 / Accepted: 12 April 2018 / Published online: 21 April 2018

Abstract

Amino-modified carbon dots (C-dots) with positively charged surface were prepared. They display strong blue fluorescence and are shown to act as quenchers of the green fluorescence of FAM-labeled ssDNA such as the F-probe used in this work that was immobilized on the C-dots. On the addition of highly negatively charged heparin (Hep), it will interact with the C-dots and displace the F-probe from C-dots. Once the F-probe is displaced by Hep, its green fluorescence is restored. The intrinsic blue fluorescence of the C-dots remains stable after addition of Hep. Thus, a signal-on ratiometric fluorometric assay was developed for the ultra-sensitive detection of Hep. The underlying mechanisms of quenching and recovery are discussed. Under optimized conditions, the recovery of the ratiometric fluorescence of the system composed of C-dots and quenched F-probe is proportional to the Hep concentration in the range of 0.01–2.0 μg·mL^{-1} (= 0.00125–0.25 U·mL^{-1}). The method was successfully applied to the determination of Hep in spiked serum samples.

Keywords Fluorescent carbon nanomaterial · ssDNA quenching platform · Fluorescence assay · Ratiometric strategy · Sensitive detection

Introduction

Heparin (Hep), a highly negatively charged glycosaminoglycan with linear structure, can be employed universally as an anticoagulant in clinical treatment, such as joint replacement. Hep can not only be used in surgeries to prevent thrombosis, but also be applied to prevent and treat arterial thromboembolism, venous thrombosis, and pulmonary embolism. The therapeutic dosage of Hep is maintained within the ranges of 2–8 U·mL^{-1} during cardiovascular surgery and 0.2–1.2 U·mL^{-1} for postoperative and long-term care [1, 2]. The control and appropriate dosage of Hep are crucial. Hep overdose results in several side effects that involve spontaneous hemorrhage. Thus, quick and facile monitoring of Hep during the therapeutic process or drug quality control is a crucial task. Numerous analytical methodologies, including the strong anion exchange-high performance liquid chromatography [3], colorimetric method based on gold nanomaterials [4] and metal organic framework nanosheets as peroxidase mimics [5], and fluorescent methods based on aggregation, have been fabricated to directly detect Hep [6–8]. Moreover, indirect methods, such as anti-factor Xa activity assay, were also applied to monitor Hep levels [9]. These methods show improved accuracy and reliability but still suffer from the disadvantages of being time consuming, complicated, and lacking sensitivity.

A fluorometric strategy based on the interaction between Hep and fluorogen is an effective approach owing to the advantages of simplicity and sensitivity [2, 6, 7]. For instance, fluorescent silicon nanoparticles are prepared for Hep assay because that Hep-induced silicon nanoparticle aggregation turns off fluorescence intensity [6]. Another signal-off fluorescent assay based on the strong affinity of protamine and Hep

Jianyong Huang and Fenglan Li contributed equally to this work.

Electronic supplementary material The online version of this article (https://doi.org/10.1007/s00604-018-2798-2) contains supplementary material, which is available to authorized users.

✉ Shaohuang Weng
shweng@fjmu.edu.cn

[1] Department of Pharmaceutical, Fujian Medical University Union Hospital, Fuzhou 350001, China

[2] Department of Pharmaceutical Analysis, School of Pharmacy, the Higher Educational Key Laboratory for Nano Biomedical Technology of Fujian Province, Fujian Medical University, Fuzhou 350122, China

was established based on the system of fluorescent silicon dots and gold nanoparticles [8]. However, the reported fluorescence sensing strategies for Hep were based on the "signal-off" approach, which may constraint the achievement of excellent analytical performance. The Hep-binding peptide was employed as raw material to synthesize a specific fluorogen-conjugated peptide, which recognized and combined with Hep to turn on the fluorescence signals [1, 2, 10]. However, the high cost of peptide and the complex synthesis are possible negative factors for the extensive application of this strategy in Hep testing. Therefore, the design and fabrication of a fluorescent approach for Hep detection with signal-on strategy is urgently needed.

Fluorescence assay platforms based on the affinity of fluorophore-labeled DNA probes on nanomaterials are powerful tools for detecting biomolecules [11, 12]. A number of nanomaterials can be used as carrier to load single-stranded DNA (ssDNA) or hairpin DNA to form fluorophore–quencher pairs through fluorescence resonance energy transfer (FRET) [13, 14]. The detecting principle of this method is mainly based on the specific action of adsorbed DNA and biomolecules to form a complex, leave the surface of the nanomaterials, and light the fluorophore [11, 12]. However, in the system of adsorbed fluorophore-labeled DNA probes and nanomaterials, the possible interaction between targets and nanomaterials was often ignored. The application of the interaction between targets and nanomaterials in the systems involving a mixture of nanomaterials and DNA may also be a new testing origin to inspire the development of new kind biosensors [15]. Liu and co-workers constructed an interesting fluorescence glucose assay based on the reaction of nanoceria and H_2O_2 to desorb and light quenched DNA from the surface of nanoceria [15]. Using the DNA as a probe, we envisage whether a new method for analytes can be established based on the interaction of analytes and nanomaterials to displace the adsorbed DNA probe. Carbon dots, a new type of fluorescent nanomaterial, garner widespread interest owing to their facile preparation, stable fluorescence property, prospects in biomedicine, and biocompatibility [16–18]. Although numerous studies about fluorescence assay on the basis of the fluorescence of carbon dots have been conducted [16–18], the use of carbon dots as an internal reference fluorescence signal and carrier for fluorophore-labeled DNA to fabricate analytical method is rare. Using an internal reference signal can be developed as ratiometric assay [19, 20] to improve the reproducibility of the sensing results, because of the avoiding of possible interferences from surrounding environment and fluctuations of probe concentration.

Herein, we design and synthesize amino-rich surface carbon dots (C-dots) through a facile heating melting method that utilizes citric acid, glutathione, and polyethylenepolyamine (PEPA) as raw materials. These C-dots, which contained abundant positively charged amino on the surface, were excellent nanoquenchers for FAM-labeled ssDNA with stable C-dots internal fluorescence. Interestingly, Hep can recover the fluorescence intensity of quenched FAM-labeled ssDNA from the complex of C-dots and FAM-labeled ssDNA. During this process, the displacement of the FAM-labeled ssDNA from C-dots by Hep attributed to electrostatic action was responsible for the recovery of FAM. This mode of action was based on the interaction of Hep and C-dots, markedly deviating from that of the common target acting on adsorbed DNA [11, 12, 14]. Furthermore, the luminous intensity of C-dots was stable with or without ssDNA and Hep. Thus, with FAM-labeled ssDNA as a probe and C-dots as the internal reference fluorescence signal, a signal-on ratiometric fluorescence assay strategy for Hep with excellent performance was developed.

Experimental

Chemicals and apparatus

The DNA sequences used in this work were synthesized and obtained from Takara Biotechnology Co., Ltd. (http://www.takarabiomed.com.cn/). FAM-labeled DNAs with different compositions and lengths, including FAM-labeled TCAACATCAGTCTGATAAGCTA (named as F-probe), FAM-A10, FAM-A20, and FAM-A40, were selected. Herein, FAM-A10 represents FAM modified DNA with 10 consecutive adenines. TAMRA-labeled A20 (TAMRA-A20) were also used. All sequences are listed from the 5′- to 3′- End. Two kinds of graphene oxide (GO) nanosheet with different sizes (GO1 > 500 nm and GO2~50–200 nm) were purchased from Nanjing XFNano Materials Technology Company (http://xf.xfnano.com/) and used as received. Heparin injection (Hep, 50 mg·mL^{-1}, 6250 U·mL^{-1}) was purchased from Chengdu Haitong Pharmaceutical Co., Ltd. (http://www.hepatunn.com/about.aspx). Hyaluronic acid (HA) was obtained from Zhejiang Jingjia Medical Technology Co.,Ltd. (http://www.hairont.com/). Bovine serum albumin (BSA), Dextran (Dex), Chondroitin sulfate (Chs), Citric Acid (CA) and Reduced Glutathione (GSH) were purchased from Aladdin Chemistry Co. Ltd. (http://www.aladdin-reagent.com/). Protamine sulfate salt and Adenosine triphosphate (ATP) were purchased from Sigma-Aldrich (https://www.sigmaaldrich.com/china-mainland.html). Fetal bovine serum (FBS) was obtained from Gibco Company (Thermo Fisher Scientific, https://www.thermofisher.com/cn/zh/home.html). All other reagents of analytical grade purchased from Sinopharm Chemical Reagent Co., Ltd. (http://www.reagent.com.cn) were used without further purification. Healthy male New Zealand white rabbits, average weight of about 2.5 kg, were obtained from the Laboratory Animal Center at Fujian Medical University (http://www.fjmu.edu.cn/). The animal

experiments were in accord with animal experiment ethics and approved by Ethics Committee for laboratory animals of Fujian Medical University.

UV-vis absorption spectra were measured on a UV-2250 spectrophotometer (Shimadzu Corporation, https://www.shimadzu.com.cn/). The Cary Eclipse Fluorescence Spectrophotometer (Agilent Technologies, https://www.agilent.com/home) was used to collect the fluorescence spectra with both excitation and emission slit widths of 5 nm. The excitation wavelength for C-dots and FAM-labeled DNAs were 345 nm and 488 nm, respectively. The emission scan range of C-dots and FAM-labeled DNAs were 378–582 nm and 508–582 nm, respectively. All UV-vis absorption and fluorescence measurements were performed at room temperature under ambient conditions. Fourier Transform Infrared Spectroscopy (FTIR) was collected using a NICOLET iS50 Infrared Spectroscopy (Thermo Fisher Scientific, https://www.thermofisher.com/cn/zh/home.html). Transmission electron microscopy (TEM) images were obtained on FEI Talos F200S (https://www.fei.com/tem/talos-f200s/?ind=MS). Zeta-potentials and dynamic light scattering (DLS) were measured on Litesizer 500 Nanometer laser particle size analyzer (Anton Paar GmbH, https://www.anton-paar.com/cn-cn/). Fluorescence anisotropy was measured on Spectrofluorometer FS5 (Edinburgh, https://www.edinst.com/products), and the detail of the calculated process of the fluorescence anisotropy value was shown in supplementary material.

Preparation of C-dots

C-dots were prepared according to our reported works [21, 22] with certain revision (Supplementary material).

Quenching behavior of C-dots toward FAM-labeled DNAs

The as-prepared C-dots at the concentration of 6.25 μg·mL^{-1} were applied to quench 50 nM FAM-labeled DNAs of different sequences in 10 mM phosphate buffered saline containing 10 mM NaCl, pH 7.4 (defined as PB saline, unless otherwise specified). The quenching efficiency (QE) was calculated by $(F_{DNA} - F_0)/F_{DNA}$, where F_0 and F_{DNA} are the fluorescence intensity of the FAM-labeled DNAs quenched or not quenched by C-dots, respectively.

Detecting performance of Hep using this method

During testing, F_0 and F are defined as the fluorescent intensity of the F-probe in the system of C-dots and F-probe (C-dots/F-probe) at 520 nm without and with the addition of Hep, respectively, unless otherwise specified. $F_{C\text{-}dots}$ is defined as the fluorescence intensity of C-dots at 425 nm.

The Hep selectivity experiments were conducted by adding 2.0 μg·mL^{-1} interferences, such as Cl^-, HCO_3^-, HPO_4^-, glucose, sodium citrate, ATP, Dex, HA, Chs, and BSA, to the mixture containing 6.25 μg·mL^{-1} C-dots and 50 nM F-probe in 10 mM PB saline (pH 7.4), respectively. Moreover, the fluorescence intensity of the C-dots/F-probe toward Hep with or without the presence of interferents was also measured and compared.

The C-dots/F-probe contained 6.25 μg·mL^{-1} C-dots and 50 nM F-probe in 200 μL of 10 mM PB saline (pH 7.4). A series of Hep solutions at different concentrations were added to the mixed solution, which was then incubated for 10 min prior to fluorometric measurements. The emission spectra of C-dots and F-probe were monitored with the excitation wavelengths of 345 and 488 nm, respectively. The detection of Hep in simulated serum samples was tested in 1% fetal bovine serum (FBS) diluted with PB saline. Other reagents and testing conditions were similar to those in the detection process in aqueous media.

Detection of Hep in real serum samples

Rabbit blood from New Zealand white rabbits was used in the preparation of rabbit serum through centrifugation at 8000 rpm for 10 min. The concentrations of Hep in the diluted rabbit serum samples were detected by the standard addition method.

Results and discussion

Characterization of C-dots

The morphology, elemental components, molecular structure, and optical properties of C-dots were studied (Fig. 1). C-dots were quasi-spherical in shape and relatively regular in size. C-dots presented a narrow distribution with average diameter of 2.50 nm and lattice parameter of 0.23 nm after calculating the all particles in Fig. 1a. The XPS result of the C-dots showed the three main element components of C, O, and N, thereby suggesting the successful doping of N. Although the original reacting material of GSH contained S, the content of the element is rare in C-dots (Fig. 1b) possibly owing to the passivation of PEPA during preparation [23]. The FTIR spectrum of the C-dots revealed that the band at 1650 cm^{-1} was attributed to the characteristic stretching vibration absorption of C=O. The strong signals at 3278 and 3423 cm^{-1} were assigned to the stretching vibration of -NH_2 and -OH, respectively. The bands at 1294 and 1140 cm^{-1} were assigned to the stretching vibration of the C-N- bonds, confirming the doping effect of N during preparation. Moreover, the observed strong peak at 1560 cm^{-1} was attributed to the N-H bending vibration, suggesting the amino-rich surface characteristic of the C-dots

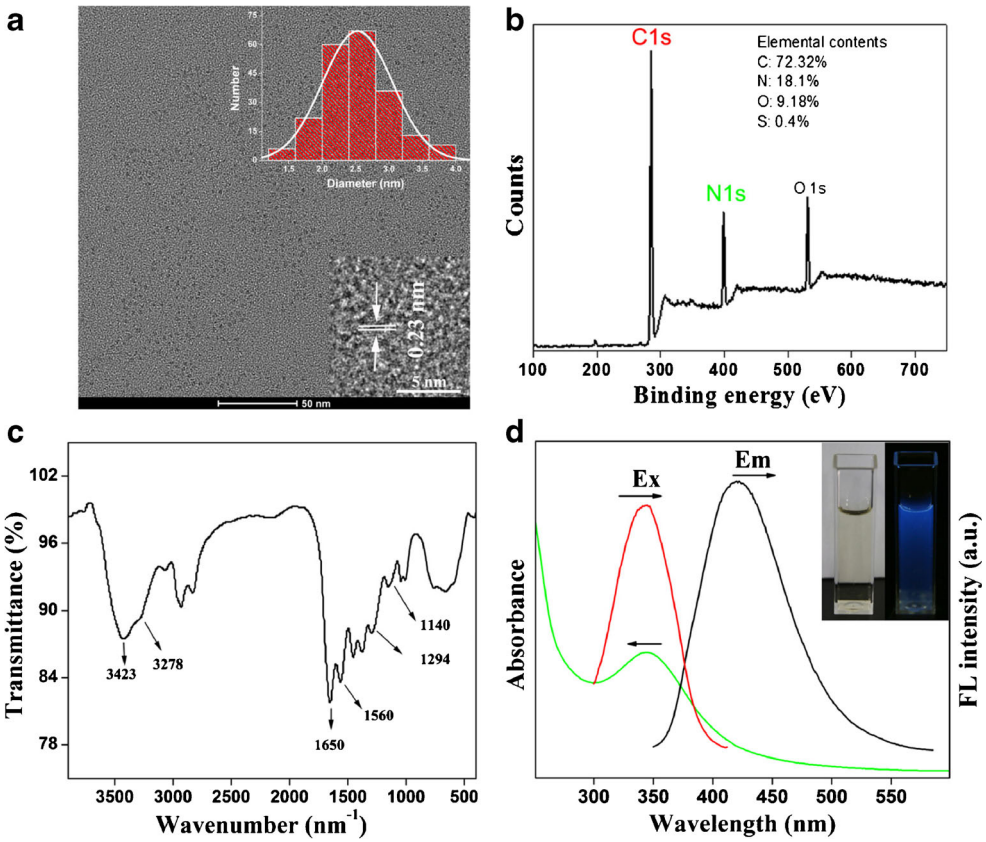

Fig. 1 TEM image (**a**), XPS survey spectrum (**b**), FTIR spectrum (**c**), and optical properties of UV–vis and fluorescent spectra (**d**) of C-dots. Inset of (**a**) is the distribution of nanoparticle sizes and HRTEM image of C-dots. Inset of (**d**) is the picture of C-dots under visible (left) and UV (right) light

[24]. The presence of amino and other hydrophilic groups was speculated to not only enhance the water solubility of C-dots (Fig. S1) but also modulate the surface charge of C-dots [25]. C-dots exhibited an evident absorption peak at around 345 nm and a maximum fluorescence emission at around 425 nm with excitation at a suitable wavelength of 345 nm, shown using UV–vis test and fluorescence measurement, respectively (Fig. 1d). Furthermore, the aqueous solution of C-dots showed blue fluorescence under UV irradiation with the absolute photoluminescence quantum yield of 12.6%. Furthermore, C-dots showed good fluorescence stability under salt conditions (Fig. S2) and photo excitation (Fig. S4), which was shown in detailed in supplementary material.

Feasibility of the detection of Hep by C-dots/F-probe

The fluorescence assay platform based on the formation of FRET pairs from fluorophore and nanomaterials has attracted extensive research interests [11]. One of the primary aims of the fluorescence assay platform is the design and preparation of a new kind of nanomaterial, such as carbon-based materials, as quenching carrier [14, 26]. Herein, the interaction between C-dots and the FAM-modified ssDNA was investigated. Considering the internal fluorescence of the C-dots, synchronous scan fluorescence spectroscopy [27], was applied to evaluate the fluorescent intensity of C-dots and F-probe in different conditions. Thus, the technique known as synchronous excitation fluorescence spectroscopy was carried out (Fig. 2). The set value of the wavelength difference

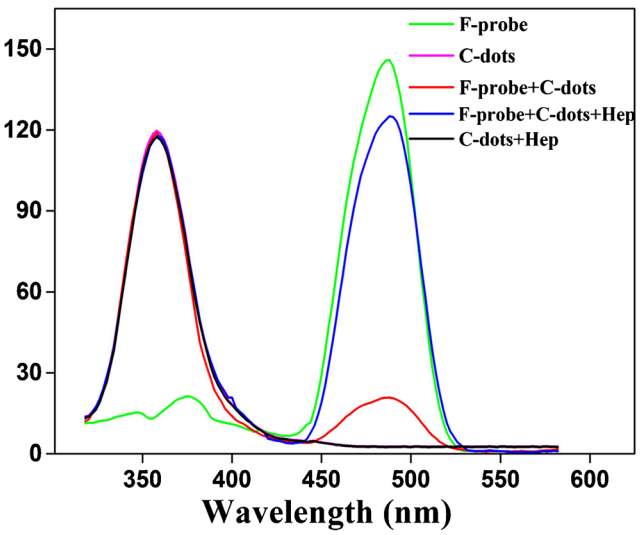

Fig. 2 Synchronous fluorescence spectra ($\Delta\lambda = 50$ nm, scan range from 320 to 582 nm) of the F-probe, C-dots, C-dots/F-probe, C-dots/F-probe + Hep and C-dots+Hep, respectively

(Δλ) between the emission and excitation wavelengths (Δλ = λem-λex) [27] was 50 nm. The C-dots with or without Hep exhibited stable intensity at the emission wavelength of 360 nm. And the emission wavelength of single F-probe was 480 nm. In the C-dots/F-probe, the emission peak at 480 nm was quenched, whereas the fluorescence emission at 360 nm attributed to the C-dots remained stable. Moreover, in the C-dots/F-probe, the added Hep recovered the quenched F-probe at 480 nm with the stable fluorescence intensity of C-dots. These results not only revealed that C-dots functioned as effective quenchers for the FAM-labeled ssDNA but also confirmed the feasibility of Hep detection by the fluorescence assay based on the C-dots/F-probe. Moreover, the stable fluorescence emission of C-dots can be applied as a reference for the variable fluorescence intensity of the F-probe controlled by Hep to be a ratiometric strategy. To the best of our knowledge, this is the first example of Hep monitoring by using a system containing C-dots and dye-labeled ssDNA through ratiometric strategy.

Principle of the assay system for Hep

The principles of fluorescence assay platform based on nanomaterials as quencher and fluorophore-labeled ssDNA are mainly ascribed to the recognition and binding of the ssDNA to the targets [11, 12]. To investigate the principle of Hep testing by using the C-dots/F-probe, we applied several other FAM-labeled DNAs with different lengths and compositions, including FAM-A10, FAM-A20, FAM-A40, and F-probe. As shown in Fig. 3a, C-dots (6.25 μg·mL^{-1}) exhibited similar QE for various FAM-modified DNAs (50 nM), indicating the strong and general quenching capacity of C-dots towards fluorophore-labeled ssDNA. Furthermore, Hep recovered all quenched probes, indicating the generality of Hep by coupling C-dots with fluorophore-labeled ssDNA. As for arbitrary DNA sequences that can be used as Hep probe, we concluded that the detection process differed from current reported assays for biomolecules constructed on nanoquenchers and special DNA probes, which were based on the interaction of the DNA probes and target biomolecules [11]. The Hep assay in this work was due to the interaction of Hep with the total mixture of C-dots and DNA probes. The diversification of the mixture of the C-dots and FAM-labeled ssDNA to Hep was further investigated through anisotropy measurement, which is a powerful tool for molecular interaction probing [28]. Figure 3b showed that the fluorescence anisotropy of the free F-probe was 0.04, whereas that of C-dots/F-probe was 0.14. These values indicated that the F-probe anchored on C-dots [28]. Moreover, the anisotropy of the mixture of C-dots, F-probe, and Hep was virtually equal to that of free DNA, suggesting that Hep made F-probe remove from C-dots [28].

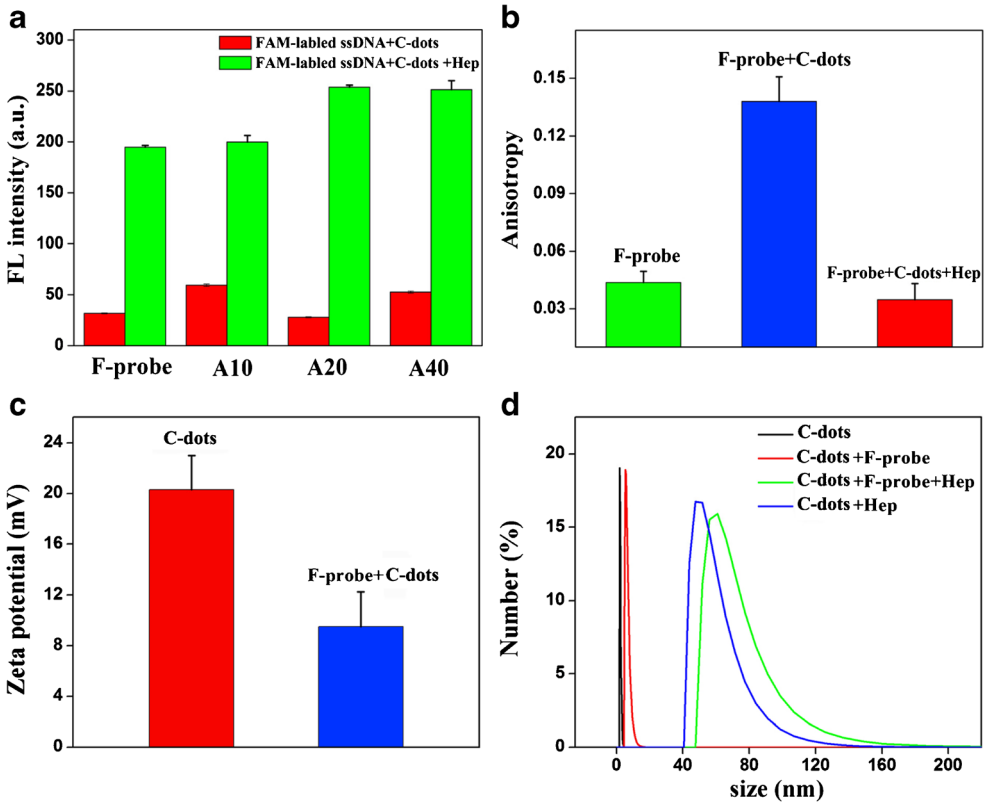

Fig. 3 **a** Quenching efficiency and fluorescence enhancement of different FAM-labeled ssDNAs quenched by C-dots with and without Hep addition. **b** Fluorescence anisotropy of the F-probe, C-dots/F-probe, and the C-dots/F-probe with the addition of Hep. **c** Zeta-potential histogram of C-dots and the C-dots/F-probe. **d** DLS of free C-dots and C-dots in the presence of F-probe, Hep, and the mixture of F-probe and Hep

In order to further investigate the underlying mechanism of the detection of heparin through the C-dots/F-probe, the famous and classical quenching example of dyes labeled ssDNA and GO was applied as a reference. As shown in Fig. S5A, with 488 nm as excitation wavelength for F-probe, the 85% QE of the C-dots for the F-probe was comparable with that of commercial large GO (GO1 > 500 nm) and slightly lower than that of small GO (GO2 ~ 50–200 nm) (Fig. S5B). It is known that the main interaction between GO and ssDNA is π-π stacking, hydrogen bonding and hydrophobic interaction [14, 28]. As shown in Fig. S5B, the introduction of Hep cannot recover the quenched F-probe by GO, suggesting that Hep didn't affect the existing interaction between GO and F-probe. Compared with the recovered fluorescence of the introduction of Hep into the C-dots/F-probe, we estimated that the removal of F-probe from C-dots by the introduction of Hep was originated some different interactions.

The effect of Hep on the C-dots/F-probe was further verified by zeta potential and DLS measurements, as shown in Fig. 3c and d. The zeta potential and size distribution of pure C-dots were measured as 20.3 mV and ca. 2.2 nm, respectively, revealing the positively charged C-dots owing to the amino-rich surface [29, 30]. However, the zeta potential of the C-dots/F-probe decreased to 9.3 mV, suggesting negative DNA binding onto positive C-dots through electrostatic interaction. The C-dots/F-probe showed particle sizes of ca. 7 nm, suggesting that aggregates of C-dots were formed through the electrostatic adherence of C-dots by using DNA. Furthermore, the measured size of the aggregates of the C-dots and Hep was ca. 50 nm, indicating that the presence of the Hep can induce the mixture of C-dots and Hep to form a large assembly (Fig. 3d). Moreover, aggregates with size of ca. 60 nm were formed through the introduction of Hep into the C-dots/F-probe, suggesting that further assembly occurred in the C-dots/F-probe with the added Hep.

Thus, the above results suggested the principle of the fluorescent assay for Hep in two steps (Scheme 1). Small size C-dots can assemble into an aggregate to load and quench FAM-labeled ssDNA through electrostatic interaction regardless of the relation of the ssDNA base sequence. As for the introduction of Hep, the highly negative Hep interacted with C-dots through the stronger electrostatic interaction between Hep and C-dots. Thus, the introduction of Hep displaced the adsorbed ssDNA from C-dots and promoted further assembly of C-dots to trigger the fluorescence of the FAM-labeled ssDNA with the stable fluorescence of C-dots. These findings indicated that the interaction between Hep and nanomaterials can be used as a testing foundation for the analytical platform of DNA-based method.

This testing process was further proven through the introduction of protamine, a proven Hep antagonist (Fig. S6). With the existence of protamine, C-dots were released from Hep because of the strong affinity of Hep and protamine. Furthermore, the positively charged C-dots again interacted with the F-probe, and the quenching of F-probe was reappeared. The results demonstrated and agreed with the discussed Hep testing principle.

Optimization of the experimental conditions (see the supplementary material for details)

Several conditions were optimized to improve the sensitivity of the ratiometric method for Hep detection. As shown in Fig. S7 and Fig. S8, pH 7.4 was chose as the suitable operating condition, 10 min was set as the suitable time for the reacting time of Hep and the C-dots/F-probe, and 6.25 $\mu g \cdot mL^{-1}$ C-dots was selected as the optimized concentration of C-dots.

Selectivity of the assay for Hep

Selectivity is an important factor for Hep detection in real applications in biological samples. Controlled experiments for possible interferences and analogues of Hep were investigated to evaluate the specificity. Figure 4a showed the changes in fluorescence intensity of F-probe after the addition of interferents and Hep into the C-dots/F-probe. Chondroitin sulfate (Chs) and hyaluronic acid (HA) share a highly similar molecular structure with Hep, but only Hep resulted in significant increase of fluorescence, whereas slightly altered fluorescence intensity for Chs can be observed. Other interfering

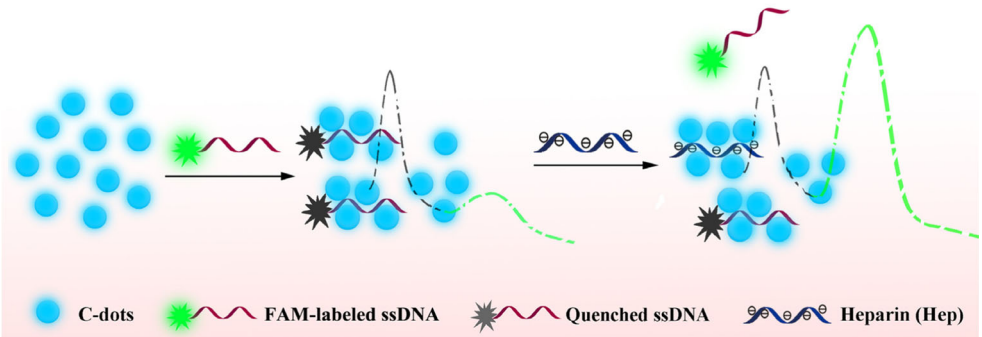

Scheme 1 Schematic of heparin (Hep) detection through the interaction of C-dots and ssDNA

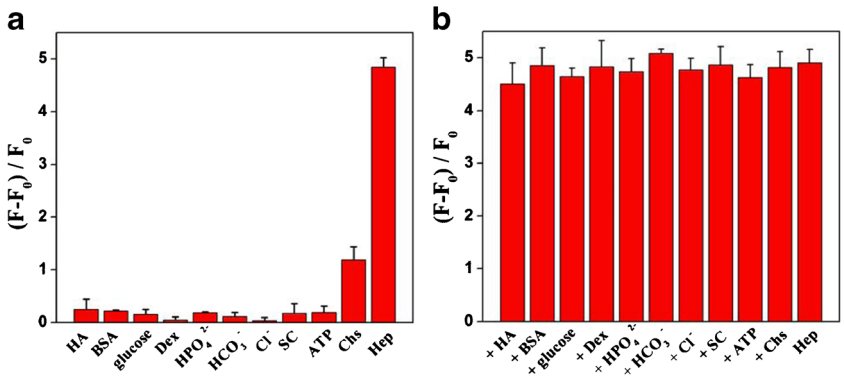

Fig. 4 **a** Fluorescent enhancing efficiency ($(F-F_0) / F_0$) of the C-dots/F-probe with the addition of Hep or other substances. **b** Fluorescence enhancing efficiency ($(F-F_0)/F_0$) of the C-dots/F-probe toward Hep and other interferents with Hep

substances containing HA exerted negligible effect on the recovered fluorescence intensity of F-probe. Competitive investigation of Hep detection in the presence of interference was further carried out to evaluate specificity (Fig. 4b). The findings demonstrated that the changed fluorescence intensities of the sensing of Hep with or without common interferents were close. It indicated that influence from interferent was negligible. These results revealed the high selectivity of this analytical method for Hep.

Detection of Hep in PB saline and simulated serum

Under the optimized conditions, the fluorescence profiles of the C-dots/F-probe were measured for variable concentration of Hep. With the increment in Hep concentration, the fluorescence of C-dots centered at 425 nm stabilized, and the fluorescence intensity of F-probe at 520 nm gradually increased (Fig. 5a). The fluorescence of F-probe (F) or the ratio ($F/F_{C\text{-}dots}$) increased with increasing concentration of Hep. Notably, a phenomenon of saturated $F/F_{C\text{-}dots}$ occurred after 2 μg/mL Hep added (Fig. 5b). This was because that the original fluorescence intensity of the added 50 nM F-probe to form the C-dots/F-probe. A linear relationship between the $F/F_{C\text{-}dots}$ and the concentration of Hep in the range of 0.01–2 $\mu g \cdot mL^{-1}$ was observed. The linear regression equation was $F/F_{C\text{-}dots} = 0.20791 + 0.52224C_{Hep\ (\mu g \cdot mL^{-1})}$ ($R^2 = 0.99796$). The calculated limit of detection (LOD) based on 3δ/s was 9.04 ng·mL^{-1}, which was markedly lower than the required

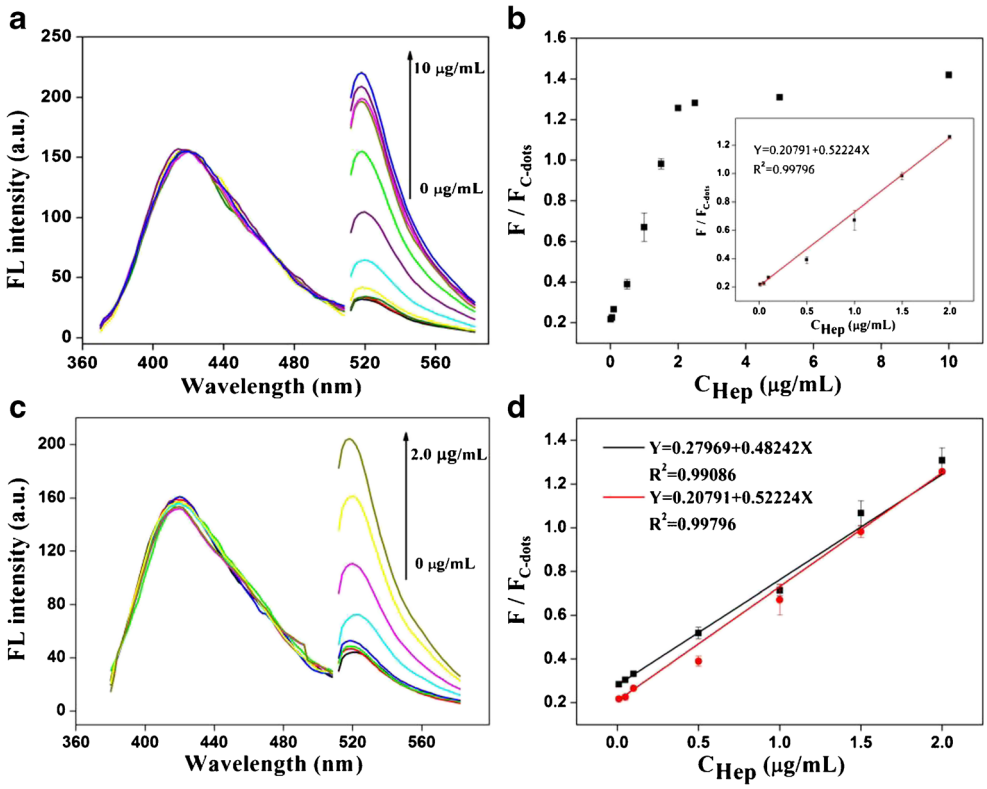

Fig. 5 Fluorescence emission spectra of the C-dots/F-probe changeed with increased Hep concentrations in PB saline (**a**) and 1% FBS (**c**). **b** Relationship and linear calibration plot (inset) between $F/F_{C\text{-}dots}$ and the concentration of Hep (0.01–2 $\mu g \cdot mL^{-1}$). **d** Comparison of the calibration curve of $F/F_{C\text{-}dots}$ to various concentrations of Hep in PBS (Red) and 1% serum (Black). Error bars are the standard deviation of three independent experiments. Herein, F is defined as the fluorescent intensity of F-probe at 520 nm, $F_{C\text{-}dots}$ is defined as the fluorescence intensity of C-dots at 425 nm

Table 1 Comparison of the reported fluorescent sensors for Heparin

Structure of the chemsensors	Response type	Dynamic range	LOD	Ref
NRCNRs and Hg^{2+} ion	Turn on	0.05–50 $\mu g \cdot mL^{-1}$	0.013 $\mu g \cdot mL^{-1}$	[31]
TPE-1	Turn on	0.32–5.5 $\mu g \cdot mL^{-1}$	3.8 $ng \cdot mL^{-1}$	[32]
H-aggregates	Turn-on	0–14 μM	52 nM	[33]
BSA-stabilized Au nanoclusters (amino-functionalized GO)	Turn-on	100 $ng \cdot mL^{-1}$ to 30 $ng \cdot mL^{-1}$	40 $ng \cdot mL^{-1}$	[34]
Z-TPE-5	Turn-on	36–180 $ng \cdot mL^{-1}$	1.53 $ng \cdot mL^{-1}$	[35]
Aminophenol-based carbon dots	Turn-off	10–100 nM	8.2 nM	[7]
SiQDs coupled with AuNPs.	Turn-off	0.002–1.4 $\mu g \cdot mL^{-1}$	0.67 $ng \cdot mL^{-1}$	[8]
Si NPs	Turn-off	0.02–2.0 $\mu g \cdot mL^{-1}$	18 $ng \cdot mL^{-1}$	[6]
GQDs and PAMAM-Gu^{+}	Turn-on (Ratiometric detection)	0.04–1.6 $\mu g \cdot mL^{-1}$	0.02 $\mu g \cdot mL^{-1}$	[36]
C-dots and FAM-labeled ssDNA	Turn-on (Ratiometric strategy)	0–2.0 μg/mL (0–0.25)	9.04 ng/mL	This work

concentration of Hep in clinical treatment of cardiovascular surgery or long-term therapy [1, 2]. In addition, the relative standard deviation (RSD) for six replicate measurements of 0.1 $\mu g \cdot mL^{-1}$ Hep was 4.7%, suggesting the good reproducibility of this method. Furthermore, we compared the analytical performance of several fluorometric assays for Hep (Table 1). Excellent linear range and LOD were obtained in the present method. Moreover, compared with the reported method based on special nanomaterials or peptides as signal source [1, 2, 5, 10], this strategy exhibited the advantages of convenience and quick operation.

Considering the need of real Hep monitoring in clinical treatment, this method was applied to test various concentrations of Hep in diluted FBS. Figure 5c showed that coupled with the stable fluorescence at 425 nm of C-dots, a similar increased fluorescence trend of F-probe observed in Fig. 5a was ascribed to the added Hep. This result suggested that the effect of composition in the serum on this method for Hep assay was disregarded. Moreover, a calibration curve with a similar slope to that of the condition in PB saline was obtained (Fig. 5d). This result suggested that the serum constituents virtually exerted slight influence on this fluorescence strategy.

Table 2 Results of heparin determination by this method in 1% rabbit serum

Sample	Added ($\mu g \cdot mL^{-1}$)	Calculated[a] ($\mu g \cdot mL^{-1}$)	Recovery (%)	RSD (%)
1	0.50	0.5598	106.6	2.58
2	1.00	0.9688	96.88	0.06
3	1.50	1.5142	101.0	0.85

[a] Average value of three independent determinations

Detection of Hep in rabbit serum samples

This method was used to determine the amount of Hep in rabbit serum samples by using the standard addition method to further evaluate the accuracy of the practical Hep assay. As listed in Table 2 and calculated from linear regression equation in PB saline, the average recoveries of Hep in rabbit serum samples reached 96.88%–106.6% with low RSD, which was acceptable for quantitative assays performed in biological samples. This outcome indicated the excellent potential applicability of this method.

Conclusions

This paper reports a novel fluorescence method for Hep detection by taking advantage of the strong electrostatic interactions between C-dots and ssDNA and the efficient contending effect of Hep to displace ssDNA. The detection process can be performed rapidly at room temperature without any catalyst or oxidizer. This method offered advantages of efficiency, convenience, and high sensitivity for Hep detection. Under the optimum condition, a good linear response for Hep detection with low detection limit was achieved. Furthermore, the method was successfully applied in the detection of Hep in real serum samples, suggesting wide clinical application in the future.

Acknowledgements The authors gratefully acknowledge for financial support from the National Natural Science Foundation of China (21405016, 21775023, 21705021), the National Science Foundation of Fujian Province (2015 J01043, 2016 J01767, 2017Y0042), the Elite Cultivation Program of Health and Family Planning of Fujian Province (2017-ZQN-61) and Opening Foundation of the State Key Laboratory of Physical Chemistry of Solid Surfaces (Xiamen University) (201517).

Compliance with ethical standards The author(s) declare that they have no competing interests.

References

1. Kim DH, Park YJ, Jung KH, Lee KH (2014) Ratiometric detection of Nanomolar concentrations of heparin in serum and plasma samples using a fluorescent Chemosensor based on peptides. Anal Chem 86:6580–6586
2. Ding Y, Shi L, Wei H (2015) A "turn on" fluorescent probe for heparin and its oversulfated chondroitin sulfate contaminant. Chem Sci 6:6361–6366
3. Han ZR, Xing XH, Yu GL, Zeng YY, Zhang LJ (2015) Heparinase digestin-based disaccharide composition analysis of heparin and heparinoid drugs. Chin J Anal Chem 43:964–970
4. Cao R, Li BX (2011) A simple and sensitive method for visual detection of heparin using positively-charged gold nanoparticles as colorimetric probes. Chem Commun 47:2865–2867
5. Cheng H, Liu Y, Hu Y, Ding Y, Lin S, Cao W, Wang Q, Wu J, Muhammad F, Zhao X, Zhao D, Li Z, Xing H, Wei H (2017) Monitoring of heparin activity in live rats using metal–organic framework Nanosheets as peroxidase mimics. Anal Chem 89: 11552–11559
6. Ma S, Chen Y, Feng J, Liu J, Zuo X, Chen X (2016) One-step synthesis of water-dispersible and biocompatible silicon nanoparticles for selective heparin sensing and cell imaging. Anal Chem 88: 10474–10481
7. Wang R, Wang X, Sun Y (2017) Aminophenol-based carbon dots with dual wavelength fluorescence emission for determination of heparin. Microchim Acta 184:187–193
8. Peng X, Long Q, Li H, Zhang Y, Yao SZ (2015) "Turn on-off" fluorescent sensor for protamine and heparin based on label-free silicon quantum dots coupled with gold nanoparticles. Sensors Actuators B 213:131–138
9. Egan G, Ensom M (2015) Measuring anti–factor Xa activity to monitor low-molecular-weight heparin in obesity: a critical review. Can J Hosp Pharm 68:33–47
10. Hu Y, Guo W, Ding Y, Cheng H, Hui Wei H (2016) Modulating luminescence of Tb^{3+}? with biomolecules for sensing heparin and its contaminant OSCS. Biosens Bioelectron 86:858–863
11. Samanta A, Medintz I (2016) Nanoparticles and DNA – a powerful and growing functional combination in bionanotechnology. Nano 8:9037–9095
12. Zhu C, Du D, Lin Y (2017) Graphene-like 2D nanomaterial-based biointerfaces for biosensing applications. Biosens Bioelectron 89: 43–55
13. Kim J, Park S, Min D (2017) Emerging approaches for graphene oxide biosensor. Anal Chem 89:232–248
14. Lu C, Liu Y, Ying YB, Liu J (2017) Comparison of MoS_2,? WS_2,? and graphene oxide for DNA adsorption and sensing. Langmuir 33: 630–637
15. Liu B, Sun Z, Huang P, Liu J (2015) Hydrogen peroxide displacing DNA from nanoceria: mechanism and detection of glucose in serum. J Am Chem Soc 137:1290–1295
16. Zu F, Yan F, Bai Z, Xu J, Wang Y, Huang Y, Zhou X (2017) The quenching of the fluorescence of carbon dots: a review on mechanisms and applications. Microchim Acta 184:1899–1914
17. Lim S, Shen W, Gao Z (2015) Carbon quantum dots and their applications. Chem Soc Rev 44:362–381
18. Zhou J, Zhou H, Tang J, Deng S, Yan F, Li W (2017) Carbon dots doped with heteroatoms for fluorescent bioimaging: a review. Microchim Acta 184:343–368
19. Cai X, Weng S, Guo R, Lin L, Chen W, Zheng Z, Huang Z, Lin X (2016) Ratiometric electrochemical immunoassay based on internal reference value for reproducible and sensitive detection of tumor marker. Biosens Bioelectron 81:173–180
20. Zhuang Y, Xu Q, Huang F, Gao P, Zhao Z, Lou X, Xia F (2016) Ratiometric fluorescent bioprobe for highly reproducible detection of telomerase in bloody urines of bladder cancer patients. ACS Sensors 1:572–578
21. Weng S, Liang D, Qiu H, Liu Z, Lin Z, Zheng Z, Liu A, Chen W, Lin X (2015) A unique turn-off fluorescent strategy for sensing dopamine based on formed polydopamine (pDA) using graphene quantum dots (GQDs) as fluorescent probe. Sensors Actuators B 221:7–14
22. Liu Z, Xiao J, Wu X, Lin L, Weng S, Chen M, Cai X, Lin X (2016) Switch-on fluorescent strategy based on N and S co-doped graphene quantum dots (N-S/GQDs) for monitoring pyrophosphate ions in synovial fluid of arthritis patients. Sensors Actuators B 229: 217–224
23. Zheng M, Liu S, Li J, Qu D, Zhao H, Guan X, Hu X, Xie Z, Jing X, Sun Z (2014) Integrating oxaliplatin with highly luminescent carbon dots: an unprecedented theranostic agent for personalized medicine. Adv Mater 26:3554–3560
24. Chung Y, Kim K, Lee B, Park C (2017) Carbon Nanodot-sensitized modulation of Alzheimer's β-amyloid self-assembly, disassembly, and toxicity. Small 13:1700983
25. Liu X, Liu J, Zheng B, Yan L, Dai J, Zhuang Z, Du J, Guo Y, Xiao D (2017) N-doped carbon dots: green and efficient synthesis on a large-scale and their application in fluorescent pH sensing. New J Chem 41:10607–10612
26. Loo AH, Sofer Z, Bousa D, Ulbrich P, Bonanni A, Pumera M (2016) Carboxylic carbon quantum dots as a fluorescent sensing platform for DNA detection. ACS Appl Mater Interfaces 8:1951–1957
27. Rubio S, Gomez-Hens A, Valcarcel M (1986) Analytical applications of synchronous fluorescence spectroscopy. Talanta 33:633–640
28. Lu CH, Yang HH, Zhu CL, Chen X, Chen GN (2009) A graphene platform for sensing biomolecules. Angew Chem Int Ed 48:4785–4787
29. Yang WQ, Ni JC, Luo F, Weng W, Wei QH, Lin ZY, Chen GN (2017) Cationic carbon dots for modification-free detection of hyaluronidase via an electrostatic-controlled ratiometric fluorescence assay. Anal Chem 89:8384–8390
30. Liu WJ, Li C, Ren YJ, Sun XB, Pan W, Li YH, Wang JP, Wang WJ (2016) Carbon dots: surface engineering and applications. J Mater Chem B 4:5772–5788
31. Wang ZX, Kong FY, Wang WJ, Zhang R, Lv WX, Yu XH, Pan HC, Wang W (2017) "OFF-ON" sensor for detecting heparin based on ?Hg^{2+}??-quenching of photoluminescence nitrogen-rich polymer carbon nanoribbons. Sensors Actuators B 242:412–417
32. Thirupathi P, Park JY, Neupane LN, Kishore MY, Lee KH (2015) Pyrene excimer-based peptidyl Chemosensors for the sensitive detection of low levels of heparin in 100% aqueous solutions and serum samples. ACS Appl Mater Interfaces 7:14243–14253
33. Mudliar NH, Singh PK (2016) Emissive H-aggregates of an ultrafast molecular rotor: a promising platform for sensing heparin. ACS Appl Mater Interfaces 8:31505–31509
34. Lan J, Zou H, Wang Q, Zeng P, Li Y, Huang C (2016) Sensitive and selective turn off-on fluorescence detection of heparin based on the energy transfer platform using the BSA-stabilized au nanoclusters/amino-functionalized graphene oxide hybrids. Talanta 161:482–488
35. Zheng J, Ye T, Chen J, Xu L, Ji X, Yang C, He Z (2017) Highly sensitive fluorescence detection of heparin based on aggregation-induced emission of a tetraphenylethene derivative. Biosens Bioelectron 90:245–250
36. Li Y, Sun H, Shi F, Cai N, Lu L, Su X (2015) Multi-positively charged dendrimeric nanoparticles induced fluorescence quenching of graphene quantum dots for heparin and chondroitin sulfate detection. Biosens Bioelectron 74:284–290